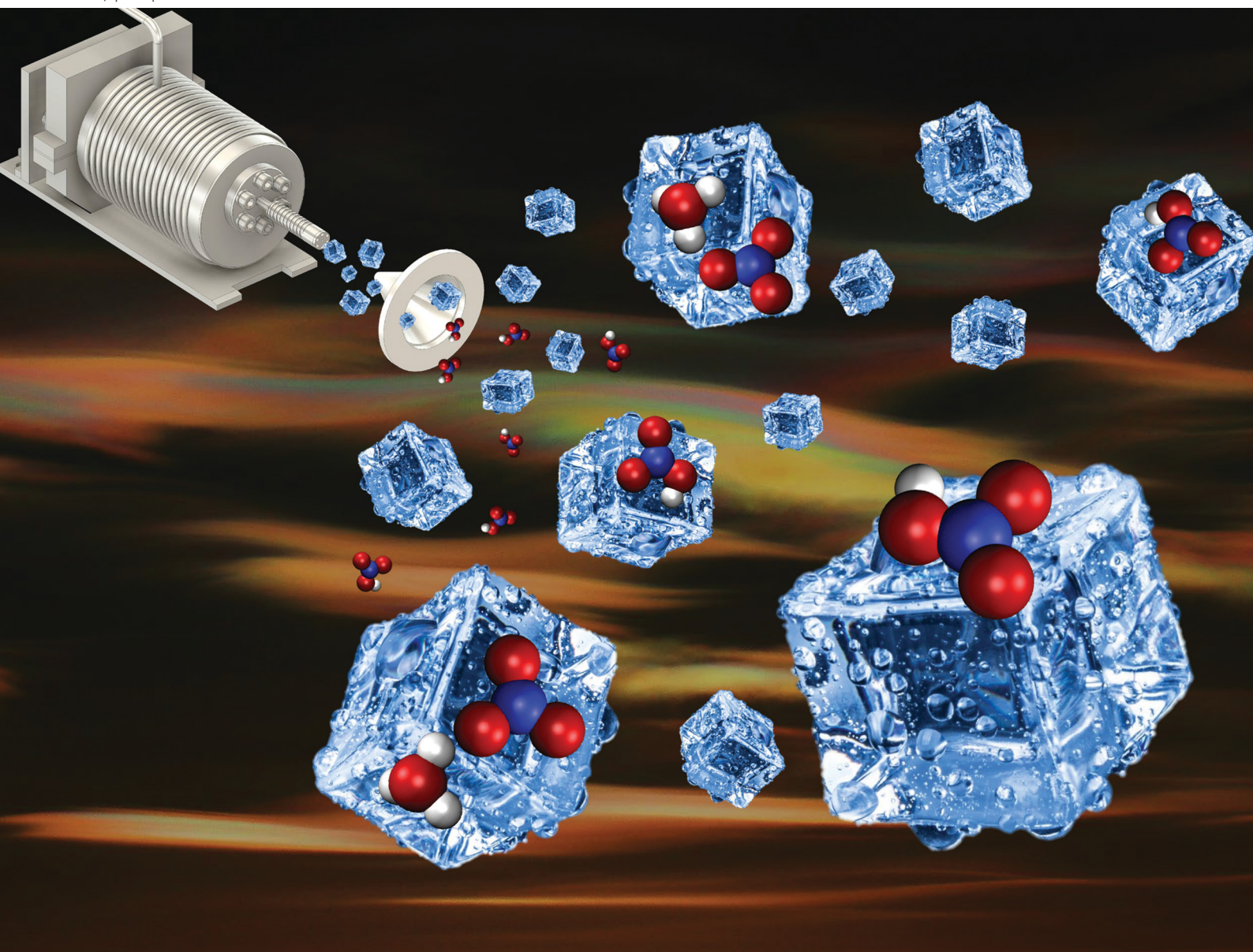


PCCP

Physical Chemistry Chemical Physics

rsc.li/pccp



ISSN 1463-9076


 Cite this: *Phys. Chem. Chem. Phys.*,
 2023, 25, 21154

Does HNO₃ dissociate on gas-phase ice nanoparticles?†

 Anastasiya Khramchenkova,^a Andriy Pysanenko,^{id}^b Jozef Ďurana,^{id}^b
 Barbora Kocábková,^{id}^b Michal Fárník^{id}^{*b} and Jozef Lengyel^{id}^{*a}

We investigated the dissociation of nitric acid on large water clusters (H₂O)_N, $\bar{N} \approx 30$ –500, *i.e.*, ice nanoparticles with diameters of 1–3 nm, in a molecular beam. The (H₂O)_N clusters were doped with single HNO₃ molecules in a pickup cell and probed by mass spectrometry after a low-energy (1.5–15 eV) electron attachment. The negative ion mass spectra provided direct evidence for HNO₃ dissociation with the formation of NO₃[−]⋯H₃O⁺ ion pairs, but over half of the observed cluster ions originated from non-dissociated HNO₃ molecules. This behavior is in contrast with the complete dissociation of nitric acid on amorphous ice surfaces above 100 K. Thus, the proton transfer is significantly suppressed on nanometer-sized particles compared to macroscopic ice surfaces. This can have considerable implications for heterogeneous processes on atmospheric ice particles.

 Received 13th June 2023,
 Accepted 11th July 2023

DOI: 10.1039/d3cp02757k

rsc.li/pccp

1 Introduction

Acid dissociation is a fundamental chemical process wherein an acid molecule releases a proton, which associates with water as an oxonium ion.^{1,2} Understanding the equilibrium involved in acid dissociation is essential for assessing the behavior of acids and their interactions with other molecules in aqueous solutions or on ice surfaces.^{1,3} Of particular significance is the study of acid dissociation on ice particles, which differs from its behavior in bulk water, as it holds substantial relevance to atmospheric phenomena.⁴ For example, ice particles containing nitric acid actively contribute to the formation of polar stratospheric clouds (PSCs) and facilitate heterogeneous reactions on their surfaces, which lead to ozone depletion in the polar regions.^{5–8} Hence, investigating factors that determine whether an acid exists in its molecular or dissociated form in/on these ices is crucial to predict the behavior of these species in the atmosphere.

Nitric acid (HNO₃) is known to be a strong acid in an aqueous solution that is essentially fully dissociated, yielding hydrated NO₃[−] and H₃O⁺ ions.⁹ Also, it acts as a strong oxidizing agent.⁹ Apart from being an essential component of PSCs, nitric acid is also involved in various other atmospheric

processes. These include the aging of naturally emitted aerosols, such as sea salt particles,^{10,11} and the formation of new particles in the upper troposphere.^{12–14} In particular, HNO₃-mediated particle formation is driven by an acid–base proton transfer, thereby enhancing particle stability and formation rate.¹⁵ Though laboratory experiments have shown particle formation based on binary HNO₃–NH₃ to be less efficient compared to H₂SO₄–NH₃,¹⁶ the slower particle formation rates with nitric acid are compensated by its significantly greater atmospheric abundance, which is several orders of magnitude higher than the concentration of sulfuric acid.¹⁷ Recent computational study has shown that nitric acid could initiate new particle formation just as well as sulfuric acid under certain conditions.¹⁸ Furthermore, the injection of HNO₃ into the H₂SO₄–NH₃ nucleation has been found to result in synergistic effects that significantly increase particle formation rates.¹⁹ Likewise, a substantial enhancement in nucleation rates by nitric acid has also been reported for the sulfuric acid–dimethylamine nucleation in the polluted boundary layer.²⁰

The dissociation mechanism of nitric acid in an aqueous solution has been the focus of many experimental and computational studies. X-ray photoelectron spectroscopy experiments have demonstrated the complete dissociation of HNO₃ in bulk water solutions, with a 20% decrease in dissociation at the liquid/vapor interface.²¹ The presence of non-dissociated nitric acid at the surface is caused by incomplete solvation.^{22–24} Further experimental evidence for this weak acid behavior at the liquid/vapour boundary has been reported using sum-frequency generation (SFG) and infrared spectroscopies.^{25–28} In general, acid dissociation equilibrium is strongly dependent on temperature, and for most acids, such as HNO₃, strong

^a Lehrstuhl für Physikalische Chemie, TUM School of Natural Sciences, Technische Universität München, Lichtenbergstraße 4, 85748 Garching, Germany. E-mail: jozef.lengyel@tum.de

^b J. Heyrovský Institute of Physical Chemistry v.v.i., Czech Academy of Sciences, Dolejškova 3, 18223 Prague, Czech Republic. E-mail: michal.farnik@jh-inst.cas.cz

† Electronic supplementary information (ESI) available: Experimental details; analysis of metastable clusters and isobaric ions; experiments with different cluster sizes and temperatures. See DOI: <https://doi.org/10.1039/d3cp02757k>



3 Experimental results

3.1 Mass spectra

Fig. 1 shows an example of the negative ion mass spectra recorded at 1.5 eV electron energy. The expansion conditions corresponded to the mean neutral cluster size of $\bar{N} \approx 180$. The top spectrum (a) shows the pure water clusters without any pickup. The spectrum exhibits only the $(\text{H}_2\text{O})_n^-$ series, attributed to the well-known low energy electron attachment to pure water clusters.⁴⁴ The $(\text{H}_2\text{O})_n\text{OH}^-$ ions are only produced by the dissociative electron attachment (DEA) at the electron energies above 6 eV. The spectrum exhibits only small fragments $n \ll \bar{N}$ due to the limited mass range dictated by the perpendicular TOF arrangement (see ESI† for explanation). The bottom spectrum (b) was recorded under the same experimental conditions with the nitric acid vapor introduced into the pickup cell. In this experiment, the pickup pressure was set so that the pickup probability for a $(\text{H}_2\text{O})_N$ cluster of an average size $\bar{N} \approx 180$ cluster was less than one to assure that we probe $\text{HNO}_3(\text{H}_2\text{O})_N$ clusters with a single HNO_3 molecule (see ESI† for the estimate of the number of adsorbed molecules). This step is crucial to avoid the contribution to NO_3^- moiety that could be generated by the reaction between OH^- and a second HNO_3 .^{38,45} Two new pronounced series occur after the pickup: the $(\text{H}_2\text{O})_n^-$ series (black open circles) is accompanied by $(\text{H}_2\text{O})_n\text{OH}^-$ (blue downward triangles), and $(\text{H}_2\text{O})_n\text{NO}_3^-$ ions (red upward triangles) appear in between the water peaks (note that the possible mass coincidences are discussed in ESI†).

The details of the mass spectra presented in Fig. 1 are depicted in Fig. 2. Upon closer investigation, the spectrum of water clusters shown in Fig. 2(a) exhibits a second series of peaks labeled by stars, which corresponds to metastable water evaporation. Observation of metastable cluster ion decay in reflectron TOF mass spectrometers for various clusters was described elsewhere,^{46,47} and the metastable fragmentation of positively charged water clusters was investigated in previous

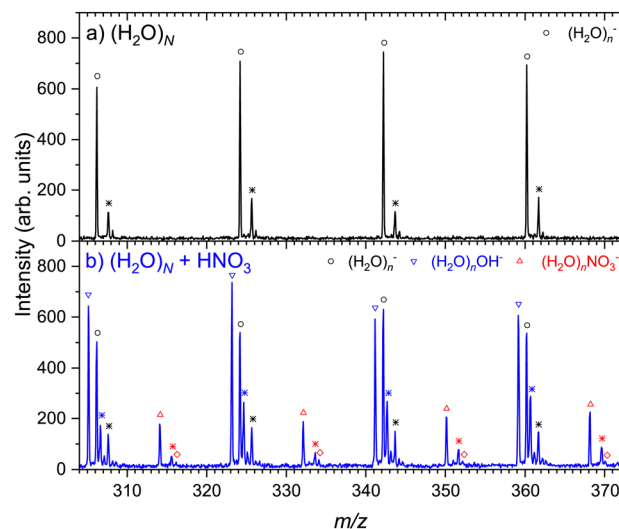


Fig. 2 Negative mass spectra at 1.5 eV for pure water (top) and with HNO_3 pickup (bottom) closeup.

studies.⁴⁸ Recently, we have investigated this effect in detail for the negatively charged pure water clusters as well, confirming the labeled peaks to be due to the metastable clusters (this point is also discussed in ESI†). In addition, there are much smaller peaks in the mass spectra corresponding to the contribution of naturally occurring isotopes.

All features present in the pure water cluster spectrum in Fig. 2(a) are reproduced in the bottom spectrum (b) after the HNO_3 pickup. Additionally, there are clearly separated $(\text{H}_2\text{O})_n\text{OH}^-$ and $(\text{H}_2\text{O})_n^-$ series, and the $(\text{H}_2\text{O})_n\text{NO}_3^-$ series. Aside these previously mentioned series, there are further peaks labeled by stars. Analogous to the pure water spectrum exhibiting metastable cluster ion fragments (black stars), the peaks labeled by blue and orange stars correspond to the metastable cluster ions in $(\text{H}_2\text{O})_n\text{OH}^-$ and $(\text{H}_2\text{O})_n\text{NO}_3^-$ series, respectively. It should be noted that even though the displacement of the metastable peak next to the $(\text{H}_2\text{O})_n\text{NO}_3^-$ ion is close to $\Delta m/z \approx 1$, it is not exactly 1 and changes slightly but regularly with m/z in accordance with the behavior of the metastable ion peaks. Thus, these peaks correspond to the metastable $(\text{H}_2\text{O})_n\text{NO}_3^-$ ions rather than $(\text{H}_2\text{O})_n\text{HNO}_3^-$ (although a small contribution of the latter ions cannot be excluded completely due to the overlap with the metastable peak). In addition, there is a very small series labeled by open red diamonds, which can be attributed to the $(\text{H}_2\text{O})_n\text{NO}_2^-$ ions. Nevertheless, their assignment is uncertain due to their low intensities and overlap with the isotope contributions. In summary, the unambiguously assigned ions resulting from the electron attachment to $(\text{H}_2\text{O})_N\text{HNO}_3$ clusters are $(\text{H}_2\text{O})_n\text{OH}^-$ and $(\text{H}_2\text{O})_n\text{NO}_3^-$.

To investigate the dependence of the observed processes on cluster size, we have measured the mass spectra for different expansion conditions corresponding to the $(\text{H}_2\text{O})_N$ cluster mean sizes from $\bar{N} \approx 30$ to 470. Qualitatively, the mass spectra are essentially the same, *i.e.*, they exhibit the same ion series (see ESI†). It ought to be mentioned that the clusters generated

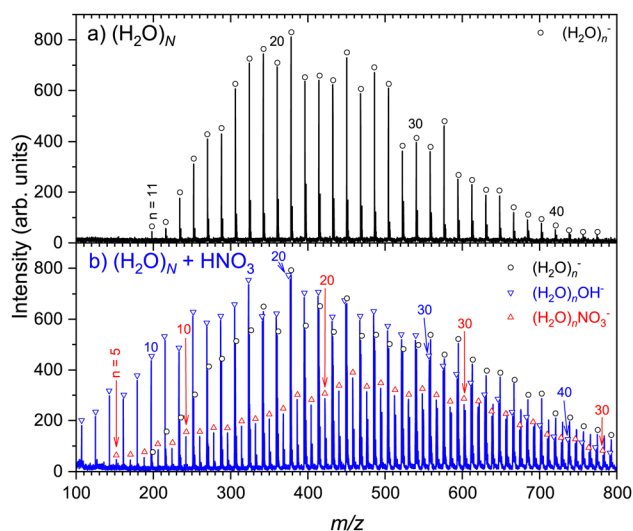


Fig. 1 Negative mass spectra at 1.5 eV for (a) pure water and (b) water with HNO_3 pickup.



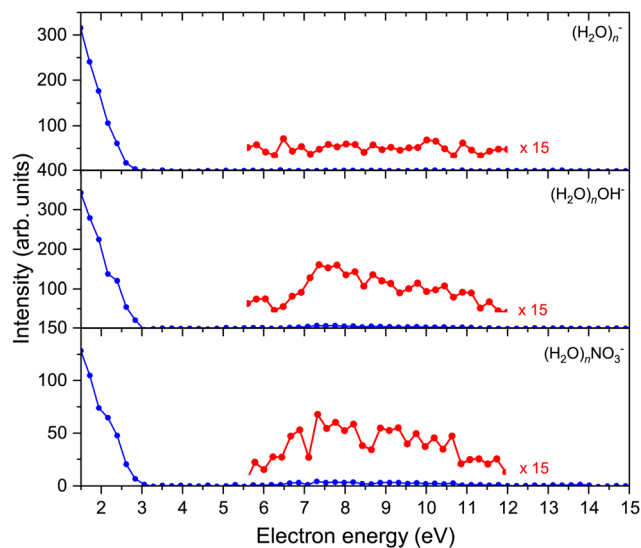


Fig. 3 Intensities of all major series in dependence of electron energy. The depicted graphs are an average of $n = 16$ – 26 spectra for a better signal-to-noise ratio.

under varying expansion conditions might have different temperatures between approximately 90 K and 180 K. However, these cluster temperatures are only approximate, based on a semiempirical model,⁴⁹ and cannot be determined experimentally. Thus, we refrain from drawing any conclusions regarding the temperature dependence of the pickup mass spectra.

3.2 Energy dependence

The above discussed spectra were recorded at the electron energy of 1.5 eV corresponding to the maximum negative ion yield. In addition, the electron energy-dependent mass spectra were measured between 0–15 eV in steps of 0.20 eV. Fig. 3 shows the electron energy dependent ion yield for selected $(\text{H}_2\text{O})_n^-$, $(\text{H}_2\text{O})_n\text{OH}^-$, and $(\text{H}_2\text{O})_n\text{NO}_3^-$ ions. The ion yield was qualitatively independent of the cluster ion size n apart from the intensity and was therefore integrated for $n = 16$ – 26 to achieve a better signal-to-noise ratio.

The spectra start at 1.5 eV since our electron gun provides reliable data above this value (see ESI[†]). Therefore, all the observed cluster ion fragments have a maximum at electron energies of 1.5 eV or lower. Upon closer look, the $(\text{H}_2\text{O})_n\text{OH}^-$ and $(\text{H}_2\text{O})_n\text{NO}_3^-$ ions exhibit a slightly increasing intensity above 6 eV. At these higher energies, OH^- can be generated by the DEA to $(\text{H}_2\text{O})_n^-$ ⁴⁴ and NO_3^- generation was observed in our previous investigation of the $(\text{HNO}_3)_m(\text{H}_2\text{O})_n$ clusters generated in co-expansion,³⁷ where the energy dependencies of individual ion yields were discussed in detail.

3.3 Co-expansion vs. pickup

We compare the present experiment to the mass spectra of the hydrated nitric acid clusters generated in co-expansion previously.^{36,37} Here, we extend the previous investigations by changing the concentration of nitric acid in a similar manner as it was done for positive ion mass spectrometry earlier.³³ To

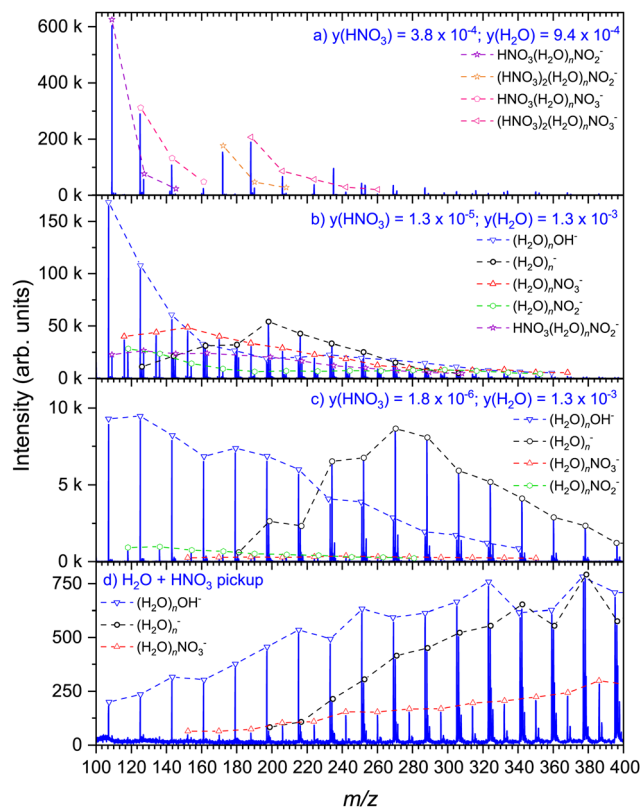


Fig. 4 Mass spectra of HNO_3 co-expansion with water (top) and of HNO_3 pickup (bottom).

this end, the nitric acid solution of known concentration is filled in the source reservoir at a constant temperature $T_R = 70$ °C, and the vapor is carried with He buffer gas at a stagnation pressure of 1 bar through the nozzle, where the hydrated HNO_3 clusters form (see ESI[†] for details). The mole fraction of HNO_3 in the vapor can be determined from acid concentration in solution, reservoir temperature, and stagnation pressure.⁵⁰

Fig. 4 shows the dependence of the mass spectra on the HNO_3 concentration in co-expansion (a)–(c) in comparison with the present pickup spectrum (d). At the highest concentration, Fig. 4(a), the spectrum is dominated by the $(\text{HNO}_3)_m(\text{H}_2\text{O})_n\text{NO}_2^-$ and $(\text{HNO}_3)_m(\text{H}_2\text{O})_n\text{NO}_3^-$ series, corresponding with observations in our previous investigation under similar conditions.³⁶ Each pronounced series contains at least one HNO_3 molecule, *i.e.*, $m \geq 1$. As the nitric acid is diluted to $y(\text{HNO}_3) = 1.3 \times 10^{-5}$, Fig. 4(b), series with $m = 0$ occur, *i.e.*, $(\text{H}_2\text{O})_n\text{NO}_2^-$ and $(\text{H}_2\text{O})_n\text{NO}_3^-$, with the latter one having a higher intensity. In contrast to the relatively abundant $\text{HNO}_3(\text{H}_2\text{O})_n\text{NO}_2^-$ ion yield in Fig. 4(a), the prevailing ions in Fig. 4(b) are $(\text{H}_2\text{O})_n\text{OH}^-$ and $(\text{H}_2\text{O})_n^-$ series. We suggest the former one originating most likely from the clusters containing a single HNO_3 molecule, and the latter one attributed to the clusters of pure water without HNO_3 . This is even more pronounced upon further dilution of the nitric acid, Fig. 4(c), where these two series are absolutely dominating the spectrum. Aside, there are minor ion series $(\text{H}_2\text{O})_n\text{NO}_2^-$ and $(\text{H}_2\text{O})_n\text{NO}_3^-$



HNO₃, but also their ionization and detection probabilities. In particular, the probability of the electron attachment to clusters with ion pairs can be significantly higher due to the ion pair dipole than to the clusters with the covalently bound molecules. Thus, the observed ratios can be interpreted qualitatively, that the acid dissociation occurs on ice nanoparticles less frequently than the non-dissociated events.

Our observation that molecular HNO₃ accounts for 50–70% of the amount present in ice nanoparticles, as determined by mass spectra (but can be even higher when the electron attachment cross section is accounted for), is notable. It is particularly interesting when compared to experiments on amorphous ice, in which substantial quantities of dissociated HNO₃ have been identified at temperatures as low as 45 K, with traces of molecular HNO₃ completely disappearing at higher temperatures of about 120 K.³⁰ In contrast to these results, our mass spectrometry analysis revealed that we primarily observe HNO₃ in its molecular form on the ice nanoparticles, even though we are far above the dissociation onset (recall the estimated cluster temperature of 90–180 K⁴⁹). In cluster experiments, the immediate environment of an HNO₃ molecule can be considered very similar to that investigated in the bulk ice studies. The structure of the ice nanoparticles is expected to be amorphous, although some crystalline core may emerge for our largest measured particle size ($\bar{N} \approx 470$).^{52,53} Unlike in macroscopic ice, the HNO₃ molecule appears to exhibit weak acid behavior when adsorbed onto ice nanoparticles. This suggests that significant size effects may occur as particles shrink to the nanometer scales, leading most likely to a kinetic inhibition of the acid dissociation.

Further, we discuss our present results in the light of the quantum chemical computations on small HNO₃(H₂O)_N clusters, which predict the onset for the HNO₃ dissociation at $N \geq 5$.³⁵ The present clusters are much larger, yet over half of the HNO₃ remains in the molecular form even when adsorbed on the clusters with an average size of about 500 molecules. The first principles molecular simulations²¹ demonstrated that complete solvation led to the dissociation, while the HNO₃ molecules at the water–air interface did not fully dissociate. They also showed that at higher concentrations, nitric acid generated hydrogen bonds without dissociating. This somewhat contradicted the structural calculations of small (HNO₃)_M(H₂O)_N clusters,³⁶ showing that even less than 5 water molecules were required for the dissociation in the clusters with $M \geq 2$. In any case, the present experiments are performed upon single collision conditions, *i.e.*, the pickup of more than one HNO₃ molecule by the cluster is unlikely. Previous molecular dynamics simulations of pickup experiments demonstrated that most dopant molecules interacted with polar water molecules upon uptake, which prevented their mobility and migration within the particle.^{54,55} The dopants remained isolated at the surface and only adjusted their orientation with respect to the neighboring water molecules. Consequently, the acid dissociation can be suppressed by the incomplete solvation in the present case. Upon collision, however, some molecules may submerge into the cluster⁵⁵ and dissociate.

Furthermore, the temperature is also a well-known factor influencing proton transfer reactions. For example, *ab initio* simulations of small hydrogen chloride–water clusters HCl(H₂O)_N with sizes at the onset of dissociation, *i.e.* $N = 4$, demonstrated that the acid dissociated and formed ion pairs at low temperatures, whereas it recombined back to the molecular form, which was more stable as the temperature increased.⁵⁶ However, for HCl adsorbed on a bulk ice the temperature trend is reversed,⁵⁷ and similar to the behavior of HNO₃ on ice discussed in the introduction. Our present case of ice nanoparticles is probably somewhere between the small clusters and bulk ice. Considering that the estimated temperatures of the larger clusters are considerably lower compared to the smaller ones (see Table S1 in ESI†),⁴⁹ it becomes apparent that the temperature may play a role in addition to the size effects. This opens up opportunities for further theoretical exploration of the interplay between cluster size and temperature on the dynamics of the acid dissociation in finite size clusters.

5 Conclusions

We have examined dissociative electron attachment of water clusters containing a single HNO₃ molecule. The aim was twofold: (i) to investigate the fundamental process of acid dissociation on an ice nanoparticle surface at a molecular level; and (ii) to mimic gas phase processes that may occur on ice particles in the atmosphere. The products were analyzed using negative ion mass spectrometry and compared to experimental results obtained with mixed nitric acid–water clusters (HNO₃)_M(H₂O)_N produced in co-expansion.

The electron attachment at 1.5 eV electron energy yielded three ion series: (1) (H₂O)_n[−] ions resulting from pure water clusters in the beam; (2) (H₂O)_nOH[−] ions originating from clusters containing a molecular HNO₃; and (3) (H₂O)_nNO₃[−] ions generated from the clusters with the NO₃[−]⋯H₃O⁺ ion pairs. We have demonstrated that the HNO₃ molecules landing on the ice nanoparticles can dissociate to a limited extent and the majority of HNO₃ molecules remains non-dissociated on the ice nanoparticles. The ice nanoparticle temperature cannot be determined exactly, however, according to various models and previous experiments,⁴⁹ it can be safely assumed between 90 and 180 K for the investigated mean cluster sizes of $\bar{N} \approx 30$ to 470. Our observations are in interesting contrast to the bulk ice experiments, where the acid dissociation occurs already at 45 K and is complete at 100–120 K. Thus, the fact that we still see non-dissociated molecules on the ice nanoparticles after about 1 millisecond of the flight time in the molecular beam speaks for a kinetic inhibition of the acid dissociation on the nanometer size ice particles.

Author contributions

AK: performed experiment and data evaluation, writing; AP: performed experiment and data evaluation; JD: helped data acquisition, review; BK: helped data acquisition, review; MF:



supervised experiment, interpretation, writing; JL: proposed idea for the experiment, interpretation, writing.

Conflicts of interest

There are no conflicts to declare.

Acknowledgements

This work was funded by the Deutsche Forschungsgemeinschaft (DFG, German Research Foundation; Project LE 4583/1-1) and Czech Science Foundation (Project 21-07062S).

References

- M. Eigen, *Angew. Chem., Int. Ed. Engl.*, 1964, **3**, 1–72.
- K. R. Leopold, *Annu. Rev. Phys. Chem.*, 2011, **62**, 327.
- D. Marx, *ChemPhysChem*, 2006, **7**, 1848–1870.
- T. Huthwelker, M. Ammann and T. Peter, *Chem. Rev.*, 2006, **106**, 1375–1444.
- T. Peter, *Annu. Rev. Phys. Chem.*, 1997, **48**, 785–822.
- S. Solomon, *Rev. Geophys.*, 1999, **37**, 275–316.
- A. J. Prenni and M. A. Tolbert, *Acc. Chem. Res.*, 2001, **34**, 545–553.
- A. R. Douglass, P. A. Newman and S. Solomon, *Phys. Today*, 2014, **67**, 42–48.
- C. Housecroft and A. G. Sharpe, *Inorganic Chemistry*, Pearson, Harlow, England, 4th edn, 2012.
- B. J. Finlayson-Pitts, *Chem. Rev.*, 2003, **103**, 4801–4822.
- Y. Liu, J. P. Cain, H. Wang and A. Laskin, *J. Phys. Chem. A*, 2007, **111**, 10026–10043.
- L. Liu, H. Li, H. Zhang, J. Zhong, Y. Bai, M. Ge, Z. Li, Y. Chen and X. Zhang, *Phys. Chem. Chem. Phys.*, 2018, **20**, 17406–17414.
- M. Kumar, H. Li, X. Zhang, X. C. Zeng and J. S. Francisco, *J. Am. Chem. Soc.*, 2018, **140**, 6456–6466.
- Y. Knattrup and J. Elm, *ACS Omega*, 2022, **7**, 31551–31560.
- C. N. Jen, P. H. McMurry and D. R. Hanson, *J. Geophys. Res.: Atmos.*, 2014, **119**, 7502–7514.
- M. Wang, W. Kong, R. Marten, X.-C. He, D. Chen, J. Pfeifer, A. Heitto, J. Kontkanen, L. Dada and A. Kürten, *et al.*, *Nature*, 2020, **581**, 184–189.
- K. Acker, D. Möller, R. Auel, W. Wipreht and D. Kalaf, *Atmos. Res.*, 2005, **74**, 507–524.
- C. J. Bready, V. R. Fowler, L. A. Juechter, L. A. Kurfman, G. E. Mazaleski and G. C. Shields, *Environ. Sci.: Atmos*, 2022, **2**, 1469–1486.
- M. Wang, M. Xiao, B. Bertozzi, G. Marie, B. Rörup, B. Schulze, R. Bardakov, X.-C. He, J. Shen and W. Scholz, *et al.*, *Nature*, 2022, **605**, 483–489.
- L. Liu, F. Yu, L. Du, Z. Yang, J. S. Francisco and X. Zhang, *Proc. Natl. Acad. Sci. U. S. A.*, 2021, **118**, e21108384118.
- T. Lewis, B. Winter, A. C. Stern, M. D. Baer, C. J. Mundy, D. J. Tobias and J. C. Hemminger, *J. Phys. Chem. C*, 2011, **115**, 21183–21190.
- E. S. Shamay, V. Buch, M. Parrinello and G. L. Richmond, *J. Am. Chem. Soc.*, 2007, **129**, 12910–12911.
- R. Bianco, S. Wang and J. T. Hynes, *J. Phys. Chem. A*, 2008, **112**, 9467–9476.
- S. Wang, R. Bianco and J. T. Hynes, *Phys. Chem. Chem. Phys.*, 2010, **12**, 8241–8249.
- C. Schnitzer, S. Baldelli, D. J. Campbell and M. J. Shultz, *J. Phys. Chem. A*, 1999, **103**, 6383–6386.
- H. Yang and B. J. Finlayson-Pitts, *J. Phys. Chem. A*, 2001, **105**, 1890–1896.
- K. A. Ramazan, L. M. Wingen, Y. Miller, G. M. Chaban, R. B. Gerber, S. S. Xantheas and B. J. Finlayson-Pitts, *J. Phys. Chem. A*, 2006, **110**, 6886–6897.
- M. C. K. Soule, P. G. Blower and G. L. Richmond, *J. Phys. Chem. A*, 2007, **111**, 3349–3357.
- J. J. Christensen, L. D. Hansen and R. M. Izatt, *Handbook of Proton Ionization Heats and Related Thermodynamic Quantities*, John Wiley and Sons, New York, 1976.
- P. Marchand, G. Marcotte and P. Ayotte, *J. Phys. Chem. A*, 2012, **116**, 12112.
- G. Marcotte, P. Ayotte, A. Bendounan, F. Sirotti, C. Laffon and P. Parent, *J. Phys. Chem. Lett.*, 2013, **4**, 2643–2648.
- B. D. Kay, V. Hermann and A. W. Castleman Jr., *Chem. Phys. Lett.*, 1981, **80**, 469.
- J. Lengyel, A. Pysanenko, J. Kočišek, V. Poterya, C. C. Pradzynski, T. Zeuch, P. Slaviček and M. Fárnik, *J. Phys. Chem. Lett.*, 2012, **3**, 3096.
- P. R. McCurdy, W. P. Hess and S. S. Xantheas, *J. Phys. Chem. A*, 2002, **106**, 7628–7635.
- J. R. Scott and J. B. Wright, *J. Phys. Chem. A*, 2004, **108**, 10578.
- J. Lengyel, M. Ončák, J. Fedor, J. Kočišek, A. Pysanenko, M. K. Beyer and M. Fárnik, *Phys. Chem. Chem. Phys.*, 2017, **19**, 11753–11758.
- J. Lengyel, J. Fedor and M. Fárnik, *Phys. Chem. Chem. Phys.*, 2019, **21**, 8691–8697.
- J. Lengyel, J. Med, P. Slaviček and M. K. Beyer, *J. Chem. Phys.*, 2017, **147**, 101101.
- M. Fárnik, *J. Phys. Chem. Lett.*, 2023, **14**, 287–294.
- A. Pysanenko, K. Fárniková, J. Lengyel, E. Pluhařová and M. Fárnik, *Environ. Sci.: Atmos*, 2022, **2**, 1292–1302.
- M. Fárnik, J. Fedor, J. Kočišek, J. Lengyel, E. Pluhařová, V. Poterya and A. Pysanenko, *Phys. Chem. Chem. Phys.*, 2021, **23**, 3195–3213.
- M. Fárnik and J. Lengyel, *Mass Spectrom. Rev.*, 2018, **37**, 630–651.
- C. Bobbert, S. Schütte, C. Steinbach and U. Buck, *Eur. Phys. J. D*, 2002, **19**, 183–192.
- M. Knapp, O. Echt, D. Kreisle and E. Recknagel, *J. Phys. Chem.*, 1987, **91**, 2601–2607.
- J. Lengyel, M. Ončák and M. K. Beyer, *Chem. – Eur. J.*, 2020, **26**, 7861–7868.
- O. Echt, P. D. Dao, S. Morgan and A. W. Castleman, *J. Chem. Phys.*, 1985, **82**, 4076–4085.
- S. Q. Wei and A. W. Castleman, *Int. J. Mass Spectrom. Ion Processes*, 1994, **131**, 233–264.



- 48 L. Belau, K. R. Wilson, S. R. Leone and M. Ahmed, *J. Phys. Chem. A*, 2007, **111**, 10075–10083.
- 49 D. Becker, C. W. Dierking, J. Suchan, F. Zurheide, J. Lengyel, M. Fárník, P. Slavíček, U. Buck and T. Zeuch, *Phys. Chem. Chem. Phys.*, 2021, **23**, 7682–7695.
- 50 G. B. Taylor, *Ind. Eng. Chem.*, 1925, **17**, 633–635.
- 51 F. C. Fehsenfeld, C. J. Howard and A. L. Schmeltekopf, *J. Chem. Phys.*, 1975, **63**, 2835–2841.
- 52 V. Buch, B. Sigurd, J. P. Devlin, U. Buck and J. K. Kazimirski, *Int. Rev. Phys. Chem.*, 2004, **23**, 375–433.
- 53 C. C. Pradzynski, R. M. Forck, T. Zeuch, P. Slavíček and U. Buck, *Science*, 2012, **337**, 1529–1532.
- 54 A. Pysanenko, A. Habartová, P. Svrčková, J. Lengyel, V. Poterya, M. Roeselová, J. Fedor and M. Fárník, *J. Phys. Chem. A*, 2015, **119**, 8991–8999.
- 55 J. Poštulka, P. Slavíček, A. Pysanenko, V. Poterya and M. Fárník, *J. Chem. Phys.*, 2022, **156**, 054306.
- 56 R. P. de Tudela and D. Marx, *Phys. Rev. Lett.*, 2017, **119**, 223001.
- 57 S.-C. Park and H. Kang, *J. Phys. Chem. B*, 2005, **109**, 5124–5132.

